JPET Fast Forward. Published on December 1, 2009 as DOI: 10.1124/jpet.109.160390




Title Page

# Three-dimensional (3D) Overlay Culture Models of Human Breast Cancer Reveal a Critical Sensitivity to MEK Inhibitors

Quanwen Li, Albert B. Chow, and Raymond R. Mattingly

Department of Pharmacology, Wayne State University School of Medicine, 540 East Canfield Ave, Detroit MI 48201

Running Title Page

Running title: MEK inhibition in 3D breast cancer model

Author for correspondence: Raymond R. Mattingly, WSU Department of Pharmacology, 540 East Canfield Ave, Detroit MI 48201. Telephone: (313) 577 6022. Fax: (313) 577 6739. E-mail: r.mattingly@wayne.edu.

Number of text pages: 28

Number of Tables: 1

Number of Figures: 5

Number of References: 30

Number of Words in Abstract: 249

Number of Words in Introduction: 430

Number of Words in Discussion: 1045

Abbreviations

rBM, reconstituted basement membrane; $GI_{50}$, concentration of drug required to inhibit growth by 50%; ERK, extracellular signal-regulated kinase

Recommended section assignment: Cellular and Molecular

Abstract

Tumor cells that are grown in three-dimensional (3D) cell culture exhibit relative resistance to cytotoxic drugs compared to their response in conventional two-dimensional (2D) culture. We studied the effects of targeted agents and doxorubicin on 2D and 3D cultures of human breast cell lines that represent the progression from normal epithelia (modeled by MCF10A cells) through hyperplastic variants to a dysplastic/carcinoma phenotype (MCF10.DCIS cells), variants transformed by expression of activated Ras, and also a basal-subtype breast carcinoma cell line (MDA-MB-231). The results showed the expected relative resistance to the cytotoxic agent doxorubicin in 3D cultures, with greater resistance in normal and hyperplastic cells than in carcinoma models. The response to the targeted inhibitors was more complex, however. Inhibition of MEK by either U0126 or CI-1040 (PD184352) produced a similar inhibition of the growth of all the MCF10 cell lines in 2D. In 3D culture, the normal and hyperplastic models exhibited some resistance, while the carcinoma models became far more sensitive to MEK inhibition. Increased sensitivity to MEK inhibition was also seen in MDA-MB-231 cells grown in 3D as compared to 2D. In contrast, inhibition of phosphatidylinositol 3'-kinase activity by wortmannin had no significant effect on the growth of any of the cells in either 2D or 3D. Our conclusion is that 3D culture models may not only model the relative resistance of tumor cells to cytotoxic therapy, but that the 3D approach may better identify the driving oncogenic pathways and critical targeted inhibitors that may be effective treatment approaches.

Introduction

Although oncogenic mutation of Ras is a relatively uncommon event in human breast cancers, there is prevalent functional activation of Ras signaling due to alterations such as over-expressed growth factor receptors (von Lintig et al., 2000; Eckert et al., 2004). Of the several pathways downstream of activated Ras, ERK MAP kinase signaling has been strongly implicated as a driver of the malignant phenotype and potential therapeutic target for breast and other cancers (McCubrey et al., 2007; Roberts and Der, 2007; McGlynn et al., 2009). Activation of this pathway may be particularly important, for example, in the basal or triple-negative subtype of breast cancer that is notably resistant to current therapies (Mirzoeva et al., 2009). Major pre-clinical and clinical effort has been focused on the MAP kinase kinases (or MEK) that are immediately upstream and critical for activation of ERK MAP kinases (Allen et al., 2003; Rinehart et al., 2004).

Most *in vitro* pre-clinical therapeutic development for carcinomas has relied on traditional cell culture systems that grow cell lines attached to dishes (2D cell culture). It has long been realized, however, that cells grown in three-dimensional (3D) matrices can show relative resistance to chemotherapeutic drugs (Weaver et al., 2002). This property has been termed multi-cellular resistance and proposed to be more representative of tumor response *in vivo* than that found in 2D cell culture (St Croix et al., 1996; Green et al., 1999; Desoize and Jardillier, 2000).

Culture of breast epithelial cells in 3D in reconstituted basement membrane (rBM) has been developed and refined by several groups, notably those of Bissell and Brugge (Debnath et al., 2003; Schmeichel and Bissell, 2003). Recently, we have adapted the rBM overlay 3D culture protocol to the MCF10 pre-malignant progression series of cells to provide an *in vitro* model of the stages of normal breast epithelia through hyperplasia, atypical hyperplasia, to ductal carcinoma *in situ* (Li et al., 2008). In this study we systematically compare the effects of MEK inhibition on 2D and 3D cultures of the MCF10 progression series, plus MCF10 variants that are transformed by high level expression of activated H-Ras and N-Ras oncogenes, and the basal breast cancer cell line MDA-MB-231. Whereas MEK inhibition has a similar inhibitory effect on all the MCF10 variant cell lines when grown in 2D culture, 3D rBM culture reveals a striking selectivity for inhibition of the carcinoma models that is in marked contrast to a relative resistance in the normal and hyperplastic models. The results from this study suggest that 3D rBM overlay culture may be an improved system for pre-clinical screening of Ras pathway inhibitors.

JPET Fast Forward. Published on December 1, 2009 as DOI: 10.1124/jpet.109.160390
This article has not been copyedited and formatted. The final version may differ from this version.



Methods

*Reagents*

Dulbecco's modified Eagle's medium (DMEM)/F12, horse serum, phosphate-buffered saline (PBS), human epithelial growth factor and insulin were purchased from Invitrogen (Carlsbad, CA). DMEM, trypsin/EDTA solution and penicillin-streptomycin were obtained from Cellgro (Herndon, VA). FBS was from Hyclone (Logan, UT). Basement membrane matrix (Matrigel) was obtained from BD Biosciences (Bedford, MA). Protease-inhibitor cocktail tablets were obtained from Roche (Indianapolis, IN). 3-(4,5-dimethylthiazol-2-yl)-2,5-diphenyltetrazolium bromide (MTT) was obtained from Molecular Probes (Eugene, OR). The MEK inhibitor PD184352 (CI-1040) [2-(2-chloro-4-iodo-phenylamino)-N-cyclopropylmethoxy-3,4-difluoro-benzamide] was generously supplied by Pfizer, Inc (New York, NY). The MEK inhibitor U0126 [1,4-diamino-2,3-dicyano-1,4-bis(2-aminophenylthio)butadiene] and its inactive analogue U0124 [1,4-diamino-2,3-dicyano-1,4-bis(methylthio)butadiene] were purchased from Calbiochem (La Jolla, CA). ECL™ Western blotting detection reagents was purchased from GE Healthcare (Buckinghamshire, UK). Doxorubicin, hydrocortisone, the PI3 kinase inhibitor wortmannin and other chemicals were from Sigma (St. Louis, MO). Rabbit anti-phospho-Akt(Ser473) and anti-total ERK1,2 antibodies were purchased from Cell Signaling Technology (Beverly, MA). Mouse anti-H-Ras antibody was from Calbiochem (La Jolla, CA). Mouse anti-N-Ras, and mouse anti-K-Ras were purchased from Santa Cruz Biotechnology (Santa Cruz, CA). Mouse anti-phospho-Erk1/2 antibody was from Sigma (St. Louis, MO). Mouse anti-tubulin antibody was obtained from Developmental Studies Hybridoma Bank (Iowa City, IA). Horseradish

peroxidase (HRP)-conjugated donkey anti-mouse IgG and HRP-conjugated donkey anti-rabbit antibodies were purchased from Jackson ImmunoResearch Laboratories, Inc. (West Grove, PA).

*Cell lines and maintenance*

MCF10A human breast epithelial progression series of cells (MCF10A, NeoT, AT1 and DCIS) were obtained from the Cell Lines Resource (Karmanos Cancer Institute, Detroit, MI). Retroviral transformed MCF10A cell lines stably expressing constitutively active H-RasD12 (H-Ras) or active N-RasD12 (N-Ras) were kind gifts from Dr. Hyeong-Reh Choi Kim in the Department of Pathology (Wayne State University). Human breast cancer cell line MDA-MB-231 was a kind gift from Dr. Bonnie F. Sloane (Wayne State University). MCF10A series of cells were maintained as monolayers at 37°C, 5% $CO_2$ in growth medium: DMEM/F12 containing 5% horse serum, 20 ng/ml EGF, 10 μg/ml insulin, 0.5 μg/ml hydrocortisone, 50 U/ml penicillin and 50 μg/ml streptomycin. MDA-MB-231 cells were maintained as monolayers in DMEM containing 10% FBS, 50 U/ml penicillin and 50 μg/ml streptomycin.

*Two-dimensional culture model and MTT assay*

Live cells can convert MTT into an insoluble dye formazan that can be solubilized by DMSO and measured using a spectrometer as an indicator of live cell numbers. These studies were performed largely as we previously described (Li et al., 2008). In brief, $10^3$ of trypsinized cells were seeded per well containing 200 μl of growth medium with inhibitors or vehicle in 96-well plates and cultured for 3 days. Then 20 μl of MTT stock solution (5 mg/ml in PBS) was added per well and the plates incubated for 4 hours. The medium was removed and the formazan

precipitate was dissolved in 150 μl of DMSO per well. The absorbance values were measured using a plate reader (SpectraFluor Plus, Tecan, Salzburg, Australia) at the wavelength of 485 nm.

*Three-dimensional cell culture model*

The 3D rBM culture model of the MCF10 variants was used as previously described (Li et al., 2008) except that the media were changed every 3 days rather than every 4 days. The 3D rBM culture of the MDA-MB-231 cells was similar except that the medium used was DMEM containing 2.5% FBS, 50 U/ml penicillin, 50 μg/ml streptomycin and supplemented with 2% (v/v) of Matrigel. After culture for 9 days, the cells were fixed with 4% paraformaldehyde for 20 minutes, quenched with 0.75% glycine in PBS for three times, 10 minutes each time, and subjected to microscopic imaging.

*Imaging and quantification of spheroidal structures*

Growth of cells in 3D rBM overlay culture can be assayed by measurement of the diameter of structures formed (Wang et al., 2002). Fixed cells were imaged with an LSM 510 confocal microscope (Zeiss, Gottingen, Germany) using a 5X objective dipping lens. Tile-scan mode was used to obtain a 5×5 phase contrast tile-image that covered the whole area of the Matrigel on a coverslip. The images were converted into TIF files with the actual image size information using the software provided by Zeiss. The diameters of the spheroidal structures were measured using Adobe Photoshop version CS2 software (Adobe Systems, Inc., San Jose, CA). Briefly, the latitudinal diameters from 100 spheroidal structures of each sample were measured in a blinded protocol relative to the experimental design.

*Statistical Analysis*

Data from the cell proliferation assays were plotted on logarithmic assays of drug concentration using Prism software (GraphPad Inc., San Diego CA) to calculate the concentration of drug required for 50% inhibition of cell growth ($GI_{50}$) by non-linear regression curve fitting with sigmoidal dose-response (variable-slope) parameter. To compare $GI_{50}$ values for statistically significant differences, the *F* test was used with a threshold of $p < 0.05$.

*Western Blot Assays*

Lysates from 2D cultures were prepared as previously described (Li and Mattingly, 2008). To obtain sufficient material for western blotting from 3D rBM cultures, the overlay culture process was adapted to be performed on 35-mm culture dishes rather than 12-mm diameter coverslips. After treatment, the cultures were briefly washed with PBS and solubilized in a buffer designed for both lysis and loading of SDS-PAGE: 50 mM Tris-HCl, pH 7.4, 100 mM NaCl, 10 mM sodium pyrophosphate, 2 mM EDTA, 1% (v/v) Nonidet P-40, 1% (v/v) 2-mercaptoethanol, 10% (v/v) glycerol, 2% (w/v) SDS, 50 mM sodium fluoride, 0.2 mM sodium orthovanadate, 0.005% (w/v) bromophenol blue and supplemented with protease inhibitor cocktails according to the manufacturer's instructions. The cell lysates were subjected to brief sonication and heated in 100 °C for 5 minutes and loaded on to SDS-PAGE gels for electrophoresis. The proteins from the gel were transferred onto nitrocellulose membrane, blocked with 2% milk solution and probed for specific target proteins with corresponding antibodies. Since protein concentrations could not be used to standardize the lysates (due to the presence of the rBM), the lysates were initially loaded based on volume and tested for content of tubulin by western blotting. If necessary, loading adjustments were made to equalize the tubulin contents of the samples.

Results

The inhibitors of MEK are among the most selective of known kinase inhibitors, and the availability of structurally distinct agents, such as CI-1040 and U0126, provides a further approach to confirm that effects are due to target block (Bain et al., 2007). We recently investigated the effects of inhibition of ERK MAP kinase activation in 2D cultures of Ras-transformed breast epithelial cells and found that it induced the re-localization of E-cadherin to cell-cell junctions (Li and Mattingly, 2008). In that study, 1 μM CI-1040 or 10 μM U0126 were sufficient to strongly inhibit ERK activation and induce reversion of transformed phenotypes, but did not lead to a complete block in cell proliferation. Since inhibition of a driving oncogenic pathway might be expected to have a more profound effect on proliferation (Sharma and Settleman, 2007), we investigated whether this result suggested that either proliferation was driven by other pathways or else that the 2D cell culture model was not the most appropriate one for these assays.

We established 3D rBM overlay cultures of MCF10A breast epithelial cells and variants that are driven by expression of activated Ras and tested for growth inhibition by inhibition of MEK, inhibition of phosphatidylinositol 3'-kinase, and by the cytotoxic agent, doxorubicin (Fig. 1). The data show that the MCF10A model of normal breast epithelial cells formed the expected acinar morphology and exhibited significant resistance to all of the targeted agents tested. The cells transformed by high-level expression of either H-Ras or N-Ras exhibited prominent but distinct hyperproliferative phenotypes in the 3D matrix. The MCF10.H-Ras cells produced extensive stellate structures, while the MCF10.N-Ras cells produced large and poorly organized

clumps of cells. In further contrast to the MCF10A cells, the H-Ras and N-Ras cells were completely inhibited in their proliferation by either of the two MEK inhibitors. As a further control we used the inactive structural analogue U1024 (Favata et al., 1998) and found that it had no effect on proliferation. The MCF10.DCIS line, which we have previously shown to have a lower level of expression of activated H-Ras than is found in the MCF10.H-Ras cells (Li and Mattingly, 2008) and a moderately dysplastic character in 3D rBM overlay culture (Li et al., 2008), showed an intermediate phenotype, with strong but incomplete inhibition of proliferation following MEK inhibition.

To check that the MEK inhibitors were fully inhibiting the target in all of the 3D rBM overlay cultures, we assayed for the levels of dually phosphorylated ERK1,2 MAP kinases. In addition to the cell lines shown in Fig. 1, we also tested the effect on the MCF10.NeoT and MCF10.AT1 variants that are intermediate in the progression series between MCF10A and MCF10.DCIS cells, and that model hyperplasia and atypical hyperplasia, respectively (Li and Mattingly, 2008). The results show that ERK1,2 MAP kinases are strongly activated in 3D rBM overlay cultures of MCF10.DCIS, MCF10.H-Ras, and MCF10.N-Ras cells, and that this activation can be completely blocked by either U0126 or CI-1040 (Fig. 2). Interestingly, levels of ERK1,2 MAP kinase activation in the MCF10A, MCF10.NeoT, and MCF10.AT1 cells were extremely low in 3D rBM overlay culture [particularly when compared to our prior results on the robust activation present in 2D culture (Li and Mattingly, 2008)], but that basal level could also be blocked by MEK inhibition.

To investigate the relative sensitivity and resistance of the MCF10A breast epithelial cells and variants to MEK inhibition in 2D and 3D culture, we defined the dose-response of growth inhibition (Figure 3). Proliferation was assayed in 2D culture by MTT assay (Li et al., 2008), while growth in 3D rBM overlay cultures was defined by measurement of the size of structures formed (Wang et al., 2002). The results showed that all of the cell lines had a similar sensitivity to growth inhibition by U0126 or CI-1040 when the cells were cultured in 2D (Fig. 3A, C). The concentration of drug required to inhibit growth by 50% ($GI_{50}$) was 1.8 – 4.4 μM for U0126, and 0.1 – 0.5 μM for CI-1040 (Table 1). There was only the most marginal trend toward the MCF10A normal cell model being slightly less sensitive than the transformed cells to MEK inhibition in 2D culture. The results of MEK inhibition on growth in the 3D rBM overlay cultures were distinct, however (Fig. 3B, D). While U0126 still blocked the proliferation MCF10.H-Ras and N-Ras cells with comparable $GI_{50}$ values to its action in 2D culture, the normal MCF10A model and the hyperplastic variants, MCF10.NeoT and MCF10.AT1, were not sensitive to this range of U0126 treatment (Table 1). The MCF10.DCIS dysplastic variant showed an intermediate response, with a partially resistant phenotype towards U0126. The results from treatment with CI-1040, which is a more potent inhibitor of ERK activation (Mattingly et al., 2006), showed even more difference in 3D rBM overlay culture from that seen in 2D culture (Fig. 3C, D). The normal MCF10A model, the hyperplastic MCF10.NeoT and MCF10.AT1 cells, and the dysplastic MCF10.DCIS cells all showed an increase in $GI_{50}$ values for growth inhibition that indicated relative resistance to CI-1040 when cultured in 3D *vs.* 2D. On the other hand, the transformed MCF10.H-Ras and N-Ras lines showed a dramatic and significant sensitization to CI-1040 inhibition, with $GI_{50}$ values reduced to the low nanomolar range (Table 1).

Since proliferation in 2D cultures had been assessed by MTT assay, whereas that in 3D cultures had been assayed by the size of structures that were formed, we further confirmed the effect of MEK inhibitors on the proliferation of the control MCF10A cells and the MCF10.H-Ras and N-Ras lines in 3D cultures by an adaptation of the MTT assay. The results (Table 2 in supplementary data) demonstrate very close alignment with those obtained by measurement of structure size (Table 1). In particular, the results confirm that MCF10.H-Ras and N-Ras cells show approximately 10-fold greater sensitivity to inhibition of proliferation by CI-1040 in 3D as compared to 2D culture, when both assays are performed using the MTT protocol after three days of treatment.

The initial studies suggested that inhibition of the phosphatidylinositol 3'-kinase pathway, which is also downstream of activated Ras, may not be required for the proliferation of the MCF10 variants in 3D rBM overlay culture (Fig. 1). Since it is important to determine whether the sensitivity of the Ras-transformed cells in 3D culture represents a general response to inhibition of several pathways or a specific reliance on ERK pathway activation, we defined the action of wortmannin in more detail (Supplementary Fig. 1). Over the range of concentrations tested, we did not find any significant growth inhibition by wortmannin on the growth of any of the MCF10 variants in either 2D or 3D rBM overlay cultures (Supplementary Fig. 1A, B). To confirm that this lack of effect was not due to a failure to inhibit the activation of the phosphatidylinositol 3'-kinase/Akt pathway, we assayed the activation of that pathway in the cells and the effect of wortmannin (Supplementary Fig. 1C). In contrast to the data on ERK activation (Fig. 2), there is increased activation of Akt (as assayed by phosphorylation of Akt at Serine-473) only in the MCF10.DCIS cell line. The MCF10.H-Ras and N-Ras lines do not have increased Akt

activation compared to that present in the normal MCF10A model or in the hyperplastic MCF10.NeoT or MCF10.AT1 variants. This pattern of Akt activation is similar between the cells grown in 2D and 3D rBM overlay culture. In all the cell lines, wortmannin was able to effectively inhibit the activation of Akt although it had no effect on cell proliferation (Supplementary Fig. 1).

Since cells derived from the breast and other tissues have typically been shown to have decreased sensitivity to growth inhibition in 3D culture conditions (St Croix et al., 1996; Green et al., 1999; Desoize and Jardillier, 2000), we further tested whether the Ras-transformed MCF10 cells in rBM overlay culture had relative sensitivity or resistance to a cytotoxic treatment. Doxorubicin is one of the most widely used chemotherapeutic drugs and has an established role in treatment of basal-subtype and triple-negative breast cancer (Schneider et al., 2008). We therefore tested the growth inhibition induced by doxorubicin in 2D and 3D cultures of the MCF10 variants (Fig. 4). In 2D culture, all of the MCF10 variants were similarly sensitive to inhibition of growth by doxorubicin, with $GI_{50}$ values between 0.4 – 2.0 μM. Once again, there was a marginal trend for the MCF10A normal model to be the least sensitive line tested. In 3D rBM overlay culture, the normal MCF10A cells (Fig. 1) and the less transformed hyperplastic and dysplastic models all exhibited significant resistance to doxorubicin (Fig. 4). $GI_{50}$ values increased to between 13.5 – 38.5 μM for inhibition of growth by doxorubicin in the MCF10A, NeoT, AT1, and DCIS cells. The MCF10.H-Ras and N-Ras cells, on the other hand, showed only a marginal resistance to doxorubicin when grown in 3D rBM overlay culture (Fig. 4). The $GI_{50}$ values slightly increased to 0.6 – 0.7 μM for inhibition of growth by doxorubicin in the MCF10.H-Ras and N-Ras cells (Table 1).

The results so far indicated that 3D rBM overlay culture revealed a relative and selective sensitization to MEK inhibition in Ras-driven MCF10 breast epithelial cells. To test whether this pattern of response was present in an independent model that includes endogenous Ras activation, we assayed the effects of MEK inhibitor and doxorubicin treatment on 2D and 3D rBM overlay cultures of MDA-MB-231 cells (Fig. 5). The results show that the MDA-MB-231 cells are relatively much more resistant to MEK inhibition in 2D culture than the MCF10 variants, with $GI_{50}$ values of 97 and 8.3 μM for U0126 and CI-1040, respectively (Table 1). These results are in close agreement with the recently published values of 60 and 33 μM (Mirzoeva et al., 2009). The change in sensitivity to MEK inhibition induced by 3D rBM overlay culture, however, was even more striking than that seen for the Ras-driven MCF10 variants (Fig. 5B). The $GI_{50}$ value for U0126 decreased to 6.3 μM, while that for CI-1040 decreased to 0.15 μM (Table 1). In comparison, the response to doxorubicin showed a modest resistance when MDA-MB-231 cells were cultured in rBM overlay culture, with $GI_{50}$ values of 16 μM in 2D and 26 μM in 3D (Table 1).

Discussion

The induction of relative resistance to growth inhibition by cytotoxic treatment when tumor cells are grown in 3D as compared to 2D culture has been generally observed and proposed to be a better model of the response of tumors to therapy *in vivo* (St Croix et al., 1996; Green et al., 1999; Desoize and Jardillier, 2000; Muir et al., 2006; Friedrich et al., 2007). Several mechanisms have been proposed to underlie this resistance, including decreased drug penetration and alterations in the signaling pathways in tumor cells that are able to form adhesion-dependent organization in 3D conditions (Green et al., 1999; Hurst et al., 2005). A classic study by Weaver et al. has previously investigated non-malignant and tumorigenic variants of HMT-3522 human breast epithelial cells for their responsiveness to a variety of pro-apoptotic treatments in 2D and 3D rBM overlay cultures. The results showed that while the non-malignant and tumor cells were similarly sensitive in 2D culture, only the normal cells became resistant when they formed organized structures in the 3D system (Weaver et al., 2002). The results in the present study on the effects of doxorubicin in the MCF10 variants and in MDA-MB-231 cells in 2D *vs.* 3D culture largely agree with these conclusions. There was a much larger increase in the $GI_{50}$ value for doxorubicin treatment of the normal and hyperplastic variants of MCF10 cells than there was for the MCF10.H-Ras, N-Ras, or MDA-MB-231 cells when cultured in 3D rBM overlay culture. In this case, relative resistance to doxorubicin correlated with a reduced activation level of ERK in the 3D system of the normal and hyperplastic models. We have previously shown that acquired resistance to doxorubicin in neuroblastoma cells is associated with decreased ERK activation (Mattingly et al., 2001). These results could therefore suggest that combinations of

kinase inhibitors that reduce ERK MAP kinase activation with doxorubicin chemotherapy may limit the efficacy of the cytotoxic component.

MEK inhibition in clinical trials has been generally well tolerated but marked by limited activity against malignancies that have included breast cancers (Rinehart et al., 2004; Adjei et al., 2008). The relative resistance of the normal MCF10A and hyperplastic models to growth inhibition by MEK inhibitors in 3D rBM overlay culture would be consistent with the lack of toxicity of this approach *in vivo*. Recently, Mirzoeva et al. have investigated MEK inhibition in a very large panel of breast cancer cell lines and concluded that a basal-like phenotype of breast cancer determines susceptibility to blockade of ERK activation (Mirzoeva et al., 2009). An implication of this result could be that a more focused clinical trial of MEK inhibitors in this particular subtype of breast cancer may be warranted. The basal subtype of breast cancer, which overlaps significantly with that defined to be "triple negative" by lack of expression of estrogen receptor, progesterone receptor and HER2, is greatly in need of effective, targeted therapeutic approaches (Schneider et al., 2008). Interestingly, the MDA-MB-231 cell line, although phenotypically basal-subtype, was paradoxically the least sensitive of all the 46 cell lines previously profiled for response to MEK inhibition (Mirzoeva et al., 2009). The very high $GI_{50}$ values found for U0126 and CI-1040 in that study are similar to those determined in this study from the 2D cultures. The great increase in potency that we found for MEK inhibitors to block the proliferation of MDA-MB-231 cells that were grown in 3D rBM overlay culture (15-fold increase in sensitivity to U0126; 56-fold increase in sensitivity to CI-1040) provides a potential explanation for this discrepancy. For example, the potent ability of CI-1040 to block MDA-MB-231 proliferation in

3D with a $GI_{50}$ value of 0.15 μM would make that cell line more sensitive than any of the 46 lines tested for inhibition in 2D culture (Mirzoeva et al., 2009).

The most striking result from the current study is that rather than showing resistance to block of ERK activation in 3D culture, the MCF10.H-Ras, MCF10.N-Ras, and MDA-MB-231 cells all show a marked sensitization to growth inhibition following treatment with MEK inhibitors in rBM overlay culture. These results are consistent with previous data on the effects of an earlier generation and less potent MEK inhibitor, PD98059, on 3D rBM cultures of breast tumor cell lines (Wang et al., 1998; Wang et al., 2002). The sensitization that we have described to MEK inhibition was highly selective since: 1, it did not occur in the MCF10A normal epithelial model or in the hyperplastic variants thereof; 2, there was no sensitivity to inhibition of the phosphatidylinositol 3'-kinase/Akt pathway that is also downstream of Ras activation; 3, the increase in sensitivity to the targeted approach in the 3D rBM overlay cultures was accompanied by the expected relative resistance to cytotoxic treatment under the same conditions. Recently a potentially similar result has also been published. Aggregates of HER2-positive SKBR-3 and SKOV-3 growing in 3D are significantly more sensitive to growth inhibition by trastuzumab than the same cell lines growing in 2D (Pickl and Ries, 2009). While we did not define a role for phosphatidylinositol 3'-kinase/Akt signaling, recent evidence suggests that combination blockade of both that pathway and MEK may be particularly effective in inhibition of basal-like breast cancers (Hoeflich et al., 2009).

In conclusion, the results of this study provide evidence that 3D overlay culture in rBM reveals a critical sensitivity to inhibition of ERK activation in two independent cell models of Ras-driven

breast cancer that is not present in 2D cell culture. In contrast to the relative resistance to cytotoxic therapeutics that is observed in 3D culture, an increase in potency of MEK inhibitors was described. The sensitivity to MEK inhibition was highly selective in that there was no sensitivity to the inhibition of the phosphatidylinoistol 3'-kinase/Akt pathway that is also downstream of Ras activation, and that normal and hyperplastic models of breast epithelia showed relative resistance to MEK inhibition in 3D culture. Thus it is reasonable to propose that 3D culture models may not only provide a better model for the relative resistance of tumor cells to cytotoxic therapy that is often found *in vivo*, but that the 3D approach may also provide a superior method to identify the driving oncogenic pathways for tumor cells and critical inhibitors that may be effective for therapeutic trial.

Acknowledgments

We thank Pfizer, Inc. for the generation gift of CI-1040.

References

Adjei AA, Cohen RB, Franklin W, Morris C, Wilson D, Molina JR, Hanson LJ, Gore L, Chow L, Leong S, Maloney L, Gordon G, Simmons H, Marlow A, Litwiler K, Brown S, Poch G, Kane K, Haney J and Eckhardt SG (2008) Phase I pharmacokinetic and pharmacodynamic study of the oral, small-molecule mitogen-activated protein kinase kinase 1/2 inhibitor AZD6244 (ARRY-142886) in patients with advanced cancers. *J Clin Oncol* **26**:2139-2146.

Allen LF, Sebolt-Leopold J and Meyer MB (2003) CI-1040 (PD184352), a targeted signal transduction inhibitor of MEK (MAPKK). *Semin Oncol* **30**:105-116.

Bain J, Plater L, Elliott M, Shpiro N, Hastie CJ, McLauchlan H, Klevernic I, Arthur JS, Alessi DR and Cohen P (2007) The selectivity of protein kinase inhibitors: a further update. *Biochem J* **408**:297-315.

Debnath J, Muthuswamy SK and Brugge JS (2003) Morphogenesis and oncogenesis of MCF-10A mammary epithelial acini grown in three-dimensional basement membrane cultures. *Methods* **30**:256-268.

Desoize B and Jardillier J (2000) Multicellular resistance: a paradigm for clinical resistance? *Crit Rev Oncol Hematol* **36**:193-207.

Eckert LB, Repasky GA, Ulku AS, McFall A, Zhou H, Sartor CI and Der CJ (2004) Involvement of Ras activation in human breast cancer cell signaling, invasion, and anoikis. *Cancer Res* **64**:4585-4592.

Favata MF, Horiuchi KY, Manos EJ, Daulerio AJ, Stradley DA, Feeser WS, Van Dyk DE, Pitts WJ, Earl RA, Hobbs F, Copeland RA, Magolda RL, Scherle PA and Trzaskos JM (1998)

Identification of a novel inhibitor of mitogen-activated protein kinase kinase. *J Biol Chem* **273**:18623-18632.

Friedrich J, Ebner R and Kunz-Schughart LA (2007) Experimental anti-tumor therapy in 3-D: spheroids--old hat or new challenge? *Int J Radiat Biol* **83**:849-871.

Green SK, Frankel A and Kerbel RS (1999) Adhesion-dependent multicellular drug resistance. *Anticancer Drug Des* **14**:153-168.

Hoeflich KP, O'Brien C, Boyd Z, Cavet G, Guerrero S, Jung K, Januario T, Savage H, Punnoose E, Truong T, Zhou W, Berry L, Murray L, Amler L, Belvin M, Friedman LS and Lackner MR (2009) In vivo antitumor activity of MEK and phosphatidylinositol 3-kinase inhibitors in basal-like breast cancer models. *Clin Cancer Res* **15**:4649-4664.

Hurst RE, Kamat CD, Kyker KD, Green DE and Ihnat MA (2005) A novel multidrug resistance phenotype of bladder tumor cells grown on Matrigel or SIS gel. *Cancer Lett* **217**:171-180.

Li Q and Mattingly RR (2008) Restoration of E-cadherin cell-cell junctions requires both expression of E-cadherin and suppression of ERK MAP kinase activation in Ras-transformed breast epithelial cells. *Neoplasia* **10**:1444-1458.

Li Q, Mullins SR, Sloane BF and Mattingly RR (2008) p21-Activated kinase 1 coordinates aberrant cell survival and pericellular proteolysis in a three-dimensional culture model for premalignant progression of human breast cancer. *Neoplasia* **10**:314-329.

Mattingly RR, Kraniak JM, Dilworth JT, Mathieu P, Bealmear B, Nowak JE, Benjamins JA, Tainsky MA and Reiners JJ, Jr. (2006) The mitogen-activated protein kinase/extracellular signal-regulated kinase kinase inhibitor PD184352 (CI-1040) selectively induces apoptosis in malignant schwannoma cell lines. *J Pharmacol Exp Ther* **316**:456-465.

Mattingly RR, Milstein ML and Mirkin BL (2001) Down-regulation of growth factor-stimulated MAP kinase signaling in cytotoxic drug-resistant human neuroblastoma cells. *Cellular Signalling* **13**:499-505.

McCubrey JA, Steelman LS, Chappell WH, Abrams SL, Wong EW, Chang F, Lehmann B, Terrian DM, Milella M, Tafuri A, Stivala F, Libra M, Basecke J, Evangelisti C, Martelli AM and Franklin RA (2007) Roles of the Raf/MEK/ERK pathway in cell growth, malignant transformation and drug resistance. *Biochim Biophys Acta* **1773**:1263-1284.

McGlynn LM, Kirkegaard T, Edwards J, Tovey S, Cameron D, Twelves C, Bartlett JM and Cooke TG (2009) Ras/Raf-1/MAPK pathway mediates response to tamoxifen but not chemotherapy in breast cancer patients. *Clin Cancer Res* **15**:1487-1495.

Mirzoeva OK, Das D, Heiser LM, Bhattacharya S, Siwak D, Gendelman R, Bayani N, Wang NJ, Neve RM, Guan Y, Hu Z, Knight Z, Feiler HS, Gascard P, Parvin B, Spellman PT, Shokat KM, Wyrobek AJ, Bissell MJ, McCormick F, Kuo WL, Mills GB, Gray JW and Korn WM (2009) Basal subtype and MAPK/ERK kinase (MEK)-phosphoinositide 3-kinase feedback signaling determine susceptibility of breast cancer cells to MEK inhibition. *Cancer Res* **69**:565-572.

Muir CP, Adams MA and Graham CH (2006) Nitric oxide attenuates resistance to doxorubicin in three-dimensional aggregates of human breast carcinoma cells. *Breast Cancer Res Treat* **96**:169-176.

Pickl M and Ries CH (2009) Comparison of 3D and 2D tumor models reveals enhanced HER2 activation in 3D associated with an increased response to trastuzumab. *Oncogene* **28**:461-468.

Rinehart J, Adjei AA, Lorusso PM, Waterhouse D, Hecht JR, Natale RB, Hamid O, Varterasian M, Asbury P, Kaldjian EP, Gulyas S, Mitchell DY, Herrera R, Sebolt-Leopold JS and Meyer MB (2004) Multicenter phase II study of the oral MEK inhibitor, CI-1040, in patients with advanced non-small-cell lung, breast, colon, and pancreatic cancer. *J Clin Oncol* **22**:4456-4462.

Roberts PJ and Der CJ (2007) Targeting the Raf-MEK-ERK mitogen-activated protein kinase cascade for the treatment of cancer. *Oncogene* **26**:3291-3310.

Schmeichel KL and Bissell MJ (2003) Modeling tissue-specific signaling and organ function in three dimensions. *J Cell Sci* **116**:2377-2388.

Schneider BP, Winer EP, Foulkes WD, Garber J, Perou CM, Richardson A, Sledge GW and Carey LA (2008) Triple-negative breast cancer: risk factors to potential targets. *Clin Cancer Res* **14**:8010-8018.

Sharma SV and Settleman J (2007) Oncogene addiction: setting the stage for molecularly targeted cancer therapy. *Genes Dev* **21**:3214-3231.

St Croix B, Rak JW, Kapitain S, Sheehan C, Graham CH and Kerbel RS (1996) Reversal by hyaluronidase of adhesion-dependent multicellular drug resistance in mammary carcinoma cells. *J Natl Cancer Inst* **88**:1285-1296.

von Lintig FC, Dreilinger AD, Varki NM, Wallace AM, Casteel DE and Boss GR (2000) Ras activation in human breast cancer. *Breast Cancer Res Treat* **62**:51-62.

Wang F, Hansen RK, Radisky D, Yoneda T, Barcellos-Hoff MH, Petersen OW, Turley EA and Bissell MJ (2002) Phenotypic reversion or death of cancer cells by altering signaling pathways in three-dimensional contexts. *J Natl Cancer Inst* **94**:1494-1503.

Wang F, Weaver VM, Petersen OW, Larabell CA, Dedhar S, Briand P, Lupu R and Bissell MJ (1998) Reciprocal interactions between beta1-integrin and epidermal growth factor receptor in three-dimensional basement membrane breast cultures: a different perspective in epithelial biology. *Proc Natl Acad Sci U S A* **95**:14821-14826.

Weaver VM, Lelievre S, Lakins JN, Chrenek MA, Jones JC, Giancotti F, Werb Z and Bissell MJ (2002) beta4 integrin-dependent formation of polarized three-dimensional architecture confers resistance to apoptosis in normal and malignant mammary epithelium. *Cancer Cell* **2**:205-216.

Footnotes

These studies were supported by grants from the Susan G. Komen Breast Cancer Foundation and National Institutes of Health [R01 CA131990]. This project was aided by the Cellular Imaging core facility that was supported by National Institutes of Health [P30 ES06639 and P30 CA22453].

Legends for Figures

Figure 1. Effects of small molecule inhibitors on the growth of MCF10 cell variants in 3D rBM overlay cultures. Cells were incubated for 9 days in 3D rBM overlay cultures under control (DMSO vehicle) or drug treatment conditions. Inhibitors used were: U0126 at 10 μM, U0124 at 10 μM, wortmannin at 200 nM; CI-1040 at 100 nM; doxorubicin at 1 μM. Phase contrast images are shown. Scale bar = 100 μm.

Figure 2. Inhibition of ERK activation by MEK inhibitors in 3D rBM overlay cultures of MCF10 cell variants. Cells were incubated for 1 day in 3D rBM overlay cultures and then either DMSO vehicle or inhibitor (10 μM U0126 or 1 μM CI-1040) was added for 24 hours as shown. Lysates were prepared and subjected to western blotting for active, dually phosphorylated ERK1/2 and for tubulin to confirm equal loading. The blots were also stripped and re-probed for total ERK1/2 as described (Mattingly et al., 2001). Results are representative of three independent experiments.

Figure 3. Dose-dependent analysis of growth inhibition of MCF10 variants by MEK inhibitors in 2D and 3D culture. (A, C) Cells were cultured in 96-well plates for 3 days with the indicated concentrations of U0126 or CI-1040 and subjected to MTT assay. (B, D) Cells were cultured for 9 days in 3D rBM overlay cultures with the indicated concentrations of U0126 or CI-1040 and the size of structures measured. The cell lines assayed were: MCF10A, black open circles; MCF10.NeoT, pink triangles; MCF10.AT1, orange triangles; MCF10.DCIS, red diamonds; MCF10.H-Ras, green circles; MCF10.N-Ras, blue squares. Data shown are mean $\pm$ SEM (n=3).

Figure 4. Dose-dependent analysis of growth inhibition of MCF10 variants by doxorubicin in 2D and 3D culture. (A) Cells were cultured in 96-well plates for 3 days with the indicated concentrations of doxorubicin and subjected to MTT assay. (B) Cells were cultured for 9 days in 3D rBM overlay cultures with the indicated concentrations of doxorubicin and the size of structures measured. The cell lines assayed were: MCF10A, black open circles; MCF10.NeoT, pink triangles; MCF10.AT1, orange triangles; MCF10.DCIS, red diamonds; MCF10.H-Ras, green circles; MCF10.N-Ras, blue squares. Data shown are mean $\pm$ SEM (n=3).

Figure 5. Dose-dependent analysis of growth inhibition of MDA-MB-231 cells in 2D and 3D culture. (A) Cells were cultured in 96-well plates for 3 days with the indicated concentrations of inhibitors and subjected to MTT assay. (B) Cells were cultured for 9 days in 3D rBM overlay cultures with the indicated concentrations of inhibitors and the size of structures measured. The inhibitors tested were: U0126, filled circle; CI-1040, open circle; doxorubicin, open triangle. Data shown are mean $\pm$ SEM (n=3).

JPET Fast Forward. Published on December 1, 2009 as DOI: 10.1124/jpet.109.160390
This article has not been copyedited and formatted. The final version may differ from this version.



Table 1. Growth Inhibition of Breast Cell Lines by MEK Inhibitors and Doxorubicin in 2D and 3D rBM Overlay Cultures

| Cell Line | $GI_{50}$ (μM) | | | | | |
|---|---|---|---|---|---|---|
| | U0126 | | CI-1040 | | Doxorubicin | |
| | 2D | 3D | 2D | 3D | 2D | 3D |
| MCF10A | 4.427 | NF | 0.482 | NF | 2.004 | 38.511 |
| MCF10.NeoT | 4.334 | NF | 0.178 | 0.587 | 0.575 | 13.518 |
| MCF10.AT1 | 1.839 | NF | 0.304 | 0.838 | 1.167 | 22.926 |
| MCF10.DCIS | 4.324 | NF | 0.107 | 0.336 | 1.439 | 27.481 |
| MCF10.H-Ras | 3.328 | 2.100 | 0.151 | 0.003* | 0.489 | 0.718 |
| MCF10.N-Ras | 2.794 | 3.740 | 0.134 | 0.002* | 0.409 | 0.627 |
| MDA-MB-231 | 96.879 | 6.325* | 8.322 | 0.148* | 16.083 | 26.140 |

NF, the data did not fit to an inhibition curve that gave a $GI_{50}$ value within the range of concentrations tested.

* $p < 0.05$ compared to corresponding value from 2D culture.

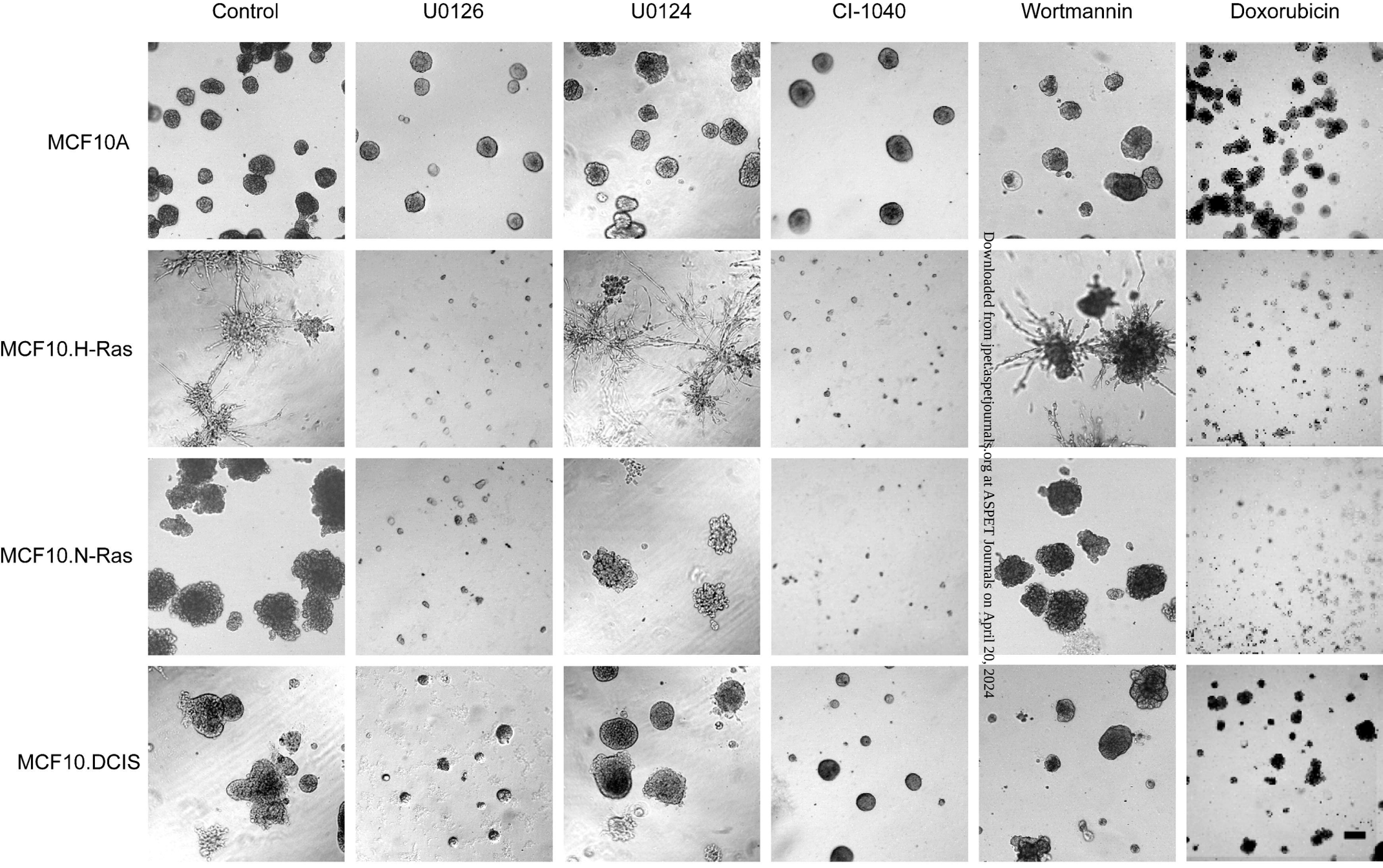




Figure 1

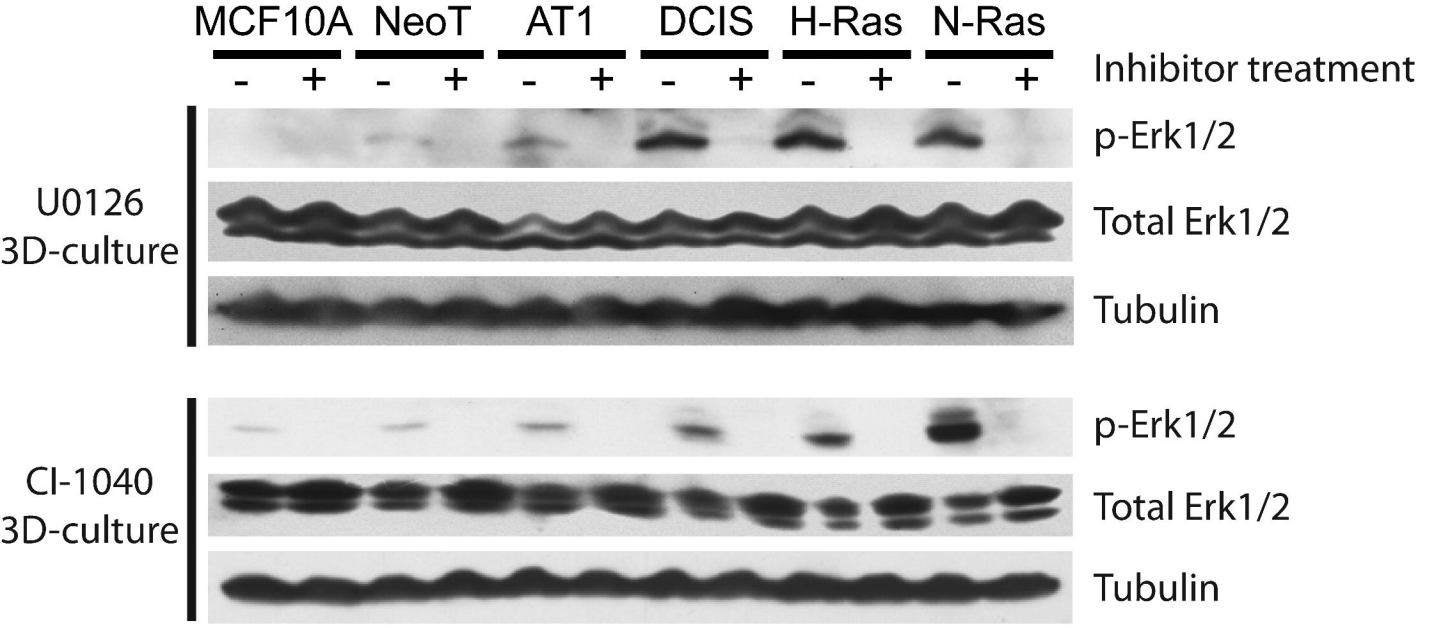
MCF10A
NeoT
AT1
DCIS
H-Ras
N-Ras
- + - + - + - + - + - +
Inhibitor treatment
U0126
3D-culture
p-Erk1/2
Total Erk1/2
Tubulin
CI-1040
3D-culture
p-Erk1/2
Total Erk1/2
Tubulin

Figure 2

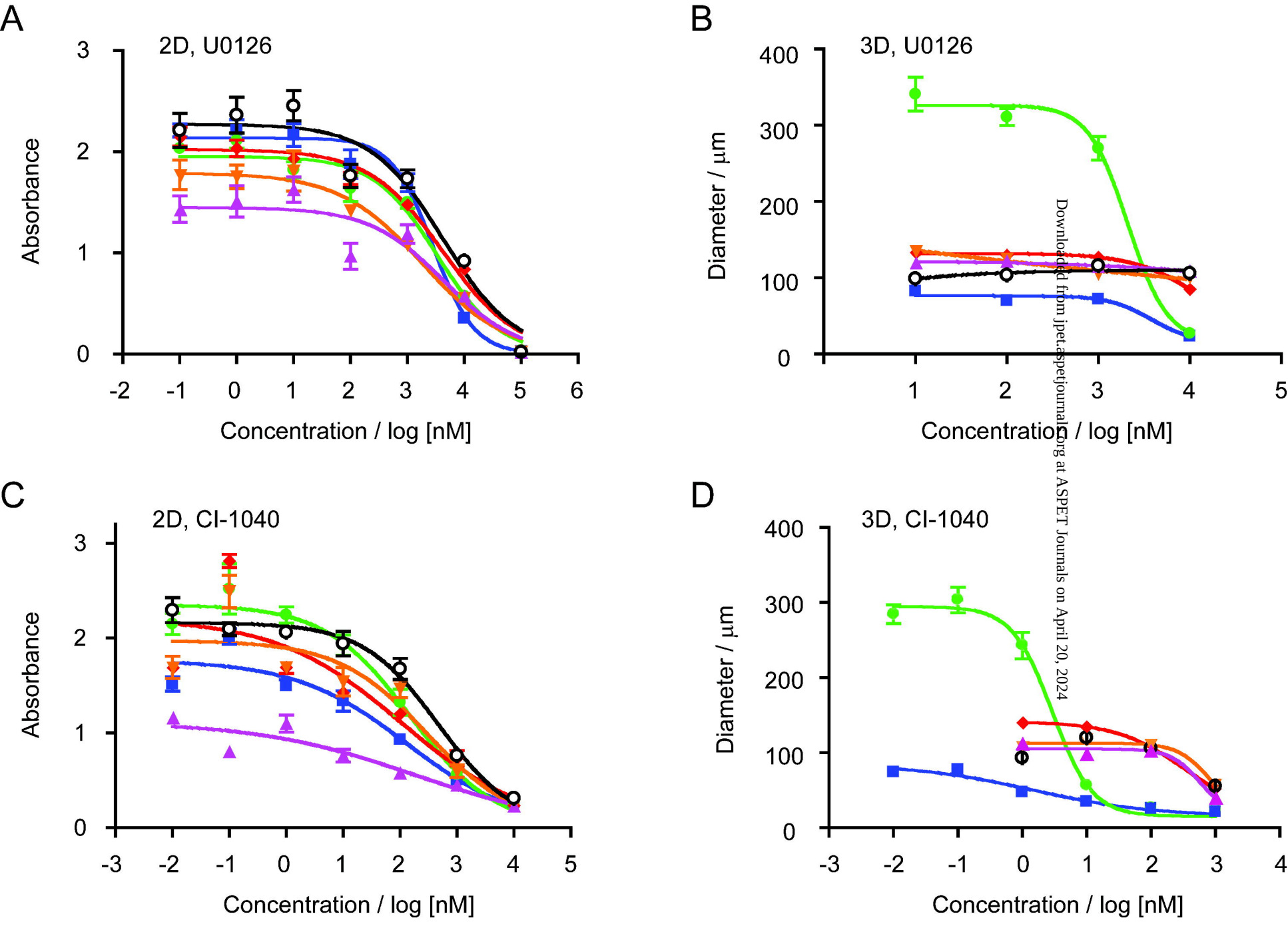




Figure 3

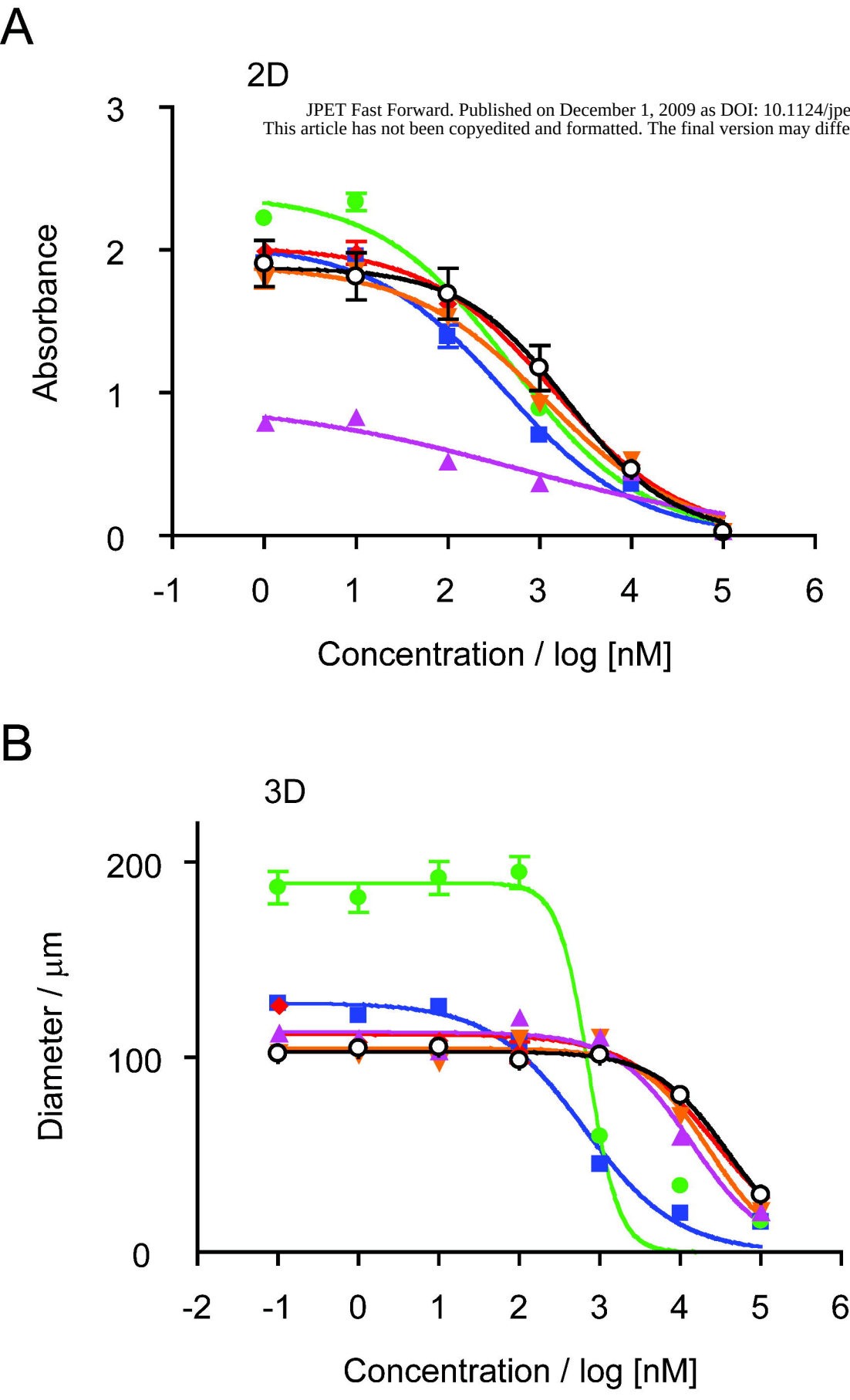


Figure 4

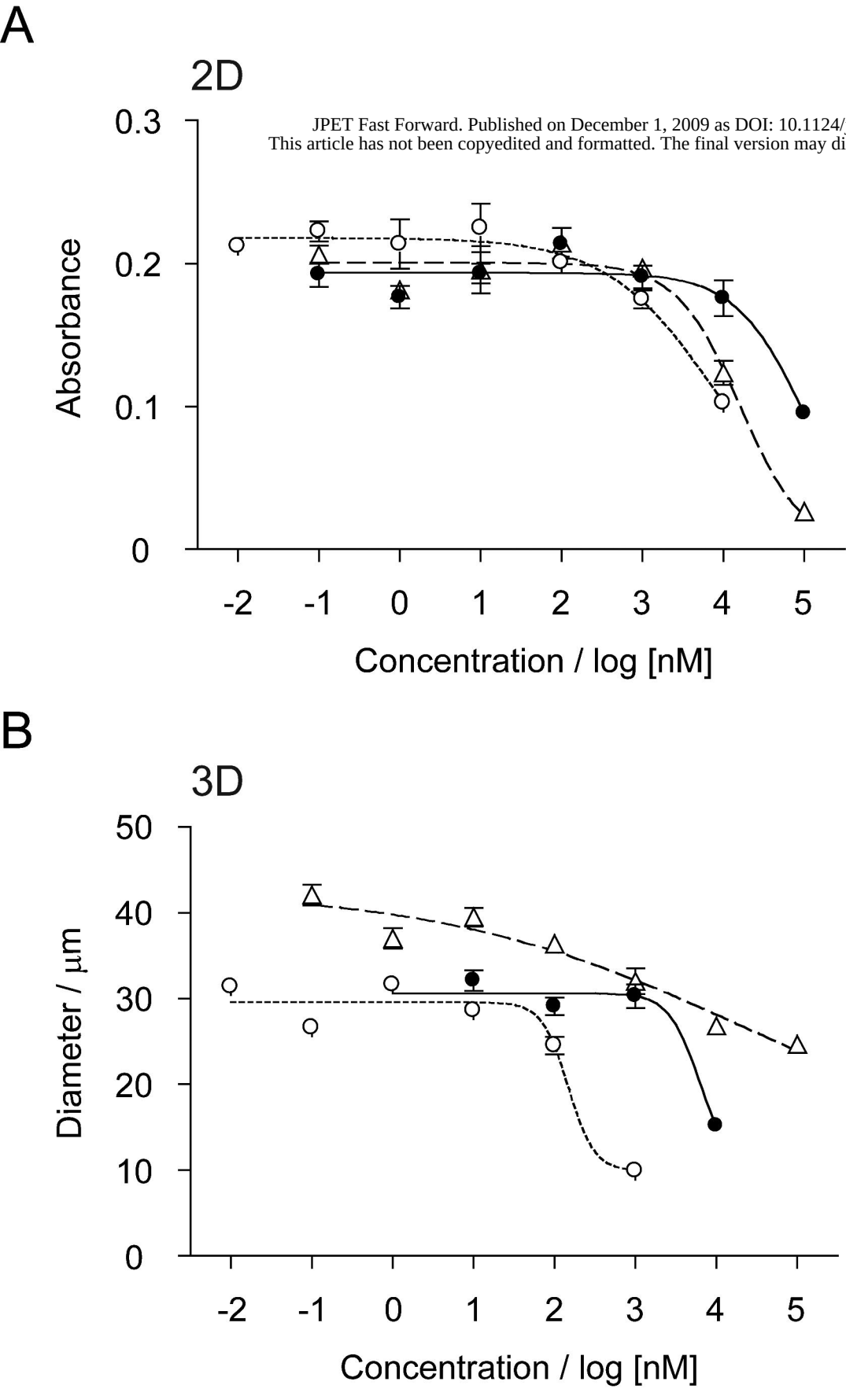


Figure 5